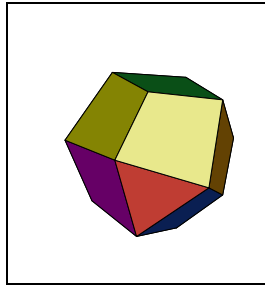


Probing Cosmic topology using CMB anisotropy

Tarun Souradeep, Dmitry Pogosyan and J. Richard Bond
*Canadian Institute for Theoretical Astrophysics,
 University of Toronto, ON M5S 3H8, Canada*



The measurements of CMB anisotropy have opened up a window for probing the global topology of the universe on length scales comparable to and beyond the Hubble radius. We have developed a new method for calculating the CMB anisotropy in models with nontrivial topology and apply it to open universe models with compact spatial topology. We conduct a Bayesian probability analysis for a selection of models which confronts the theoretical pixel-pixel temperature correlation function with the COBE-DMR data. Our results demonstrate that strong constraints on compactness arise: if the universe is small compared to the ‘horizon’ size, correlations appear in the maps that are irreconcilable with the observations.

The remarkable degree of isotropy of the cosmic microwave background (CMB) points to homogeneous and isotropic Friedmann-Robertson-Walker (FRW) models for the universe. This argument is a purely local one and does not refer to the global topological structure of the universe. In fact, in the absence of spatially inhomogeneous perturbations, a FRW model predicts an isotropic CMB regardless of the global topological structure. However, the observed large scale structure in the universe and CMB anisotropy allude to the existence of small spatially inhomogeneous primordial perturbations. The global topology of the universe does affect the observable properties of the CMB anisotropy. In compact universe models, the finite spatial size usually implies a suppression of the power in large scale perturbations and consequently the CMB anisotropy is suppressed on angular scales above a characteristic angle related to size of the universe. Another signature is the breaking of statistical isotropy in characteristic patterns determined by the photon geodesic structure of the compact manifold.

Much recent astrophysical data suggest the cosmological density parameter, Ω_0 , is subcritical.¹ In the absence of a cosmological constant, this would imply a hyperbolic spatial geometry for the universe (commonly referred to as the ‘open’ universe in cosmological literature). The topologically trivial (simply connected) hyperbolic 3-space, \mathcal{H}^3 , is non-compact and has infinite size. There are numerous theoretical motivations, however, to favor a spatially compact

universe.² To reconcile this with a flat or hyperbolic geometry, consideration of models with non-trivial topology is required. A compact cosmological model is constructed by identifying points on the standard infinite flat or hyperbolic FRW space under the action of a suitable discrete subgroup, Γ , of the full isometry group, G , of the FRW space. The FRW spatial hypersurface is the *universal cover*, tiled by copies of the compact space, \mathcal{M} . Any point \mathbf{x} of the compact space has an image $\mathbf{x}_i = \gamma_i \mathbf{x}$ in each tile on the universal cover, where $\gamma_i \in \Gamma$.

For Gaussian perturbations, the angular correlation function, $C(\hat{q}, \hat{q}')$, of the CMB temperature fluctuations in two directions \hat{q} and \hat{q}' in the sky completely encodes the CMB anisotropy predictions of a model. The dominant contribution to the anisotropy in the CMB temperature measured with wide-angle beam ($\theta_{\text{FWHM}} \gtrsim 2^\circ \Omega_0^{1/2}$) comes from the cosmological metric perturbations through the Sachs-Wolfe effect. The angular correlation function of the CMB anisotropy, $C(\hat{q}, \hat{q}')$, depends on the spatial two point correlation function, $\xi_\Phi \equiv \langle \Phi(\mathbf{x}, \tau_{\text{rec}}) \Phi(\mathbf{x}', \tau_{\text{rec}}) \rangle$ of the gravitational potential, Φ , on the hypersurface of last scattering.^a To calculate the spatial correlation function on a compact hyperbolic (CH) manifold, described by the corresponding Γ , we have developed a general technique – the *method of images*, which evades the difficult problem^b of solving for eigenfunctions of the Laplacian on these manifolds.³ Using the method of images, the spatial correlation function, ξ_Φ^c , between two points \mathbf{x} and \mathbf{x}' on a compact space of volume $V_{\mathcal{M}}$ can be expressed as⁴

$$\xi_\Phi^c(\mathbf{x}, \mathbf{x}') = \lim_{r_* \rightarrow \infty} \sum_{r_j < r_*} \xi_\Phi^u(r_j) - \frac{4\pi}{V_{\mathcal{M}}} \int_0^{r_*} dr \sinh^2 r \xi_\Phi^u(r), \quad r_j = d(\mathbf{x}, \gamma_j \mathbf{x}'). \quad (1)$$

a regularized sum over the correlation function, ξ_Φ^u , on the universal cover evaluated between \mathbf{x} and images $\gamma_i \mathbf{x}'$ of \mathbf{x}' . Numerically it suffices to evaluate the above expression up to r_* a few times the curvature radius, d_c , to reach a convergent result. We then integrate ξ_Φ^c along photon trajectories to get $C(\hat{q}, \hat{q}')$ which includes both surface and integrated (ISW) Sachs-Wolfe effects.

The CMB photons can be viewed as propagating to the observer from a 2-sphere of radius, R_H , – the sphere of last scattering (SLS). In contrast to the topologically trivial models, widely separated pixels in compact spaces can still have strong correlations if in the sum over images, eq. (1), one of the images of \mathbf{x}' happens to be close to \mathbf{x} . The dependence of the spatial correlations on the anisotropic distribution of images leads to a characteristic statistical anisotropy in the CMB in compact models. These effects are pronounced when the compact space fits well within the SLS, but persist at an observable level even when $V_{\mathcal{M}}$ is comparable to (or somewhat bigger than) V_{SLS} , the volume of SLS. If SLS does not fit completely inside a single tile – a copy of the compact space, the CMB temperature values will be identical along pairs of circles if temperature fluctuations are dominated by the surface terms at the SLS.⁵ This pattern of matched circles is one specific manifestation of the angular patterns in $C(\hat{q}, \hat{q}')$.

Figure 1 compares theoretical realizations of the CMB anisotropy in a selection of CH models with the COBE–DMR data. In this work, the six COBE–DMR four-year maps⁶ are first compressed into a (A+B)(31+53+90 GHz) weighted-sum map, with the customized Galactic cut advocated by the DMR team. There is no effective loss of information when we do further data compression by using $5.2^\circ \times 5.2^\circ$ pixels.⁷ The theory and data maps have been postprocessed so as to facilitate a fair visual comparison. The incompatibility of models with small $V_{\mathcal{M}}/V_{\text{SLS}}$ (SCH- $\Omega_0 = 0.3, 0.6$) is visually obvious: the best fit amplitudes are high which is reflected in the steeper hot and cold features. Although, SCH- $\Omega_0 = 0.9$ and LCH- $\Omega_0 = 0.6$ do not appear grossly inconsistent, the intrinsic anisotropic correlation pattern is at odds with the data.

^a Other effects which contribute to the CMB anisotropy at smaller angular scales can also be approximated in terms of spatial correlation of quantities defined on the hypersurface of last scattering.⁴

^bThe correlation function is usually computed using a mode function expansion. However, obtaining closed form expressions for eigenfunctions of the Laplacian may not be possible beyond the simplest topologies and even numerical estimation is known to be difficult in CH spaces.

We have carried out a full Bayesian analysis of the probability of the CH models given the COBE–DMR 4yr data. In Table 1 we present the *relative likelihood* of the selected models to that of the infinite, \mathcal{H}^3 , model with the same Ω_0 . (The COBE data alone does not strongly differentiate between the infinite hyperbolic models with different Ω_0 .) The anisotropy of the theoretical $C(\hat{q}, \hat{q}')$ causes the likelihood of compact models to vary significantly with the orientation of the space with respect to the sky, depending on how closely the features in the single data realization available match (or mismatch) the pattern in $C(\hat{q}, \hat{q}')$. Some optimal orientations may also have the “ugly” correlation features hidden in the Galactic cut. We analyzed 24 different orientations for each of our models and found that only the model with $V_{\mathcal{M}} > V_{\text{SLS}}$ (LCH- $\Omega_0 = 0.8$) cannot be excluded (at one orientation this model is even preferable to standard CDM; this raises a question of the statistical significance of any detection of intrinsic anisotropy of a space when only a single realization of data is available).

Similar conclusions were reached by some of the authors (JRB, DP and I. Sokolov⁸) for flat toroidal models. Comparison of the full angular correlation with COBE data led to a much stronger limit on the compactness of the universe than limits from other methods.⁹ The main result of the analysis was that $V_{\text{SLS}}/V_{\mathcal{M}} < 0.4$ at 95% *CL* for the equal-sided 3-torus. For non compact 1-torus, the constraint on the most compact dimension is not quite as strong.

In summary, our results demonstrate that the COBE data can put strong constraints on the compact models of the universe. If the universe is small compared to the ‘horizon’ size, correlations appear in the maps that are irreconcilable with the large angle COBE–DMR data.

Table 1: The Log-likelihoods of the compact hyperbolic models relative to the infinite models with same Ω_0 are listed below. The likelihoods are calculated by comparison with COBE–DMR data. The three columns of Log-likelihood ratios correspond to the best, second best and worst values that we have obtained amongst 24 different rotations of the compact space relative to the sky. The number in brackets gives a convenient, albeit crude, translation to gaussian likelihood. Only the last model can be reconciled with the COBE–DMR data.

Topology	Ω_0	$V_{\text{SLS}}/V_{\mathcal{M}}$	Relative Log. Likelihood (Gaussian approx.)		
			Orientation		
			‘best’	‘second best’	‘worst’
$m004(-5, 1)$	0.3	153.4	-35.5 (8.4 σ)	-35.7 (8.4 σ)	-57.9 (10.8 σ)
	0.6	19.3	-22.9 (6.8 σ)	-23.3 (6.8 σ)	-49.4 (9.9 σ)
	0.9	1.2	-4.4 (3.0 σ)	-8.5 (4.1 σ)	-37.4 (8.6 σ)
$v3543(2, 3)$	0.6	2.9	-3.6 (2.7 σ)	-5.6 (3.3 σ)	-31.0 (7.9 σ)
$V_{\mathcal{M}}/d_c^3 = 6.45$	0.8	0.6	2.5 (2.2 σ)	-0.8 (1.3 σ)	-12.6 (5.0 σ)

References

1. Dekel, A., Burnstein, D., & White, S.D.M. 1996, in *Critical Dialogues in Cosmology*, ed. N.Turok, (World Scientific).
2. Ellis, G.F.R. 1971, *Gen. Rel. Grav.*, **2**, 7; Lachieze-Rey, M. & Luminet, J.-P. 1995, *Phys. Rep.*, **25**, 136; Cornish, N. J., Spergel, D. N. & Starkman, G. D. 1996, *Phys. Rev. Lett.* **77**, 215
3. Bond, J. R., Pogosyan, D. & Souradeep, T. 1998, in: *Proceedings of the XVIIIth Texas Symposium on Relativistic Astrophysics*, ed. A. Olinto, J. Frieman & D. N. Schramm, (World Scientific).
4. Bond, J. R., Pogosyan, D. & Souradeep, T. 1998, *Class. Quantum Grav.* (in press), *Proc. CWRU conference on ‘Cosmology and Topology’*; *ibid.*, preprint.
5. Cornish, N. J., Spergel, D. N. & Starkman, G. D. 1996, preprint gr-qc/9602039.
6. Bennett, C. *et al* 1996, *Ap. J. Lett.*, **464**, L1; and 4-year DMR references therein.
7. Bond, J. R. 1994, *Phys. Rev. Lett.*, **74**, 4369.
8. Bond, J. R. 1997, in *Proc. of the XVIIth Moriond Astrophysics Meeting*, ed. F. R. Bouchet *et al.*, (Editions Frontieres, France); Bond, J. R. 1998, *Proc. Natl. Acad. Sci. USA*, **95**, 35.
9. Sokolov, I.Y. 1993, *JETP Lett.* **57**, 617; Starobinsky, A.A. 1993, *JETP Lett.* **57**, 622; Stevens, D., Scott, D. & Silk, J. 1993, *Phys. Rev. Lett.* **71**, 20; de Oliveira Costa, A. & Smoot, G.F. 1995, *Ap.J.* **448**, 477; de Oliveira Costa, A., Smoot, G.F. & Starobinsky, A.A. 1996, *Ap.J.* **468**, 457

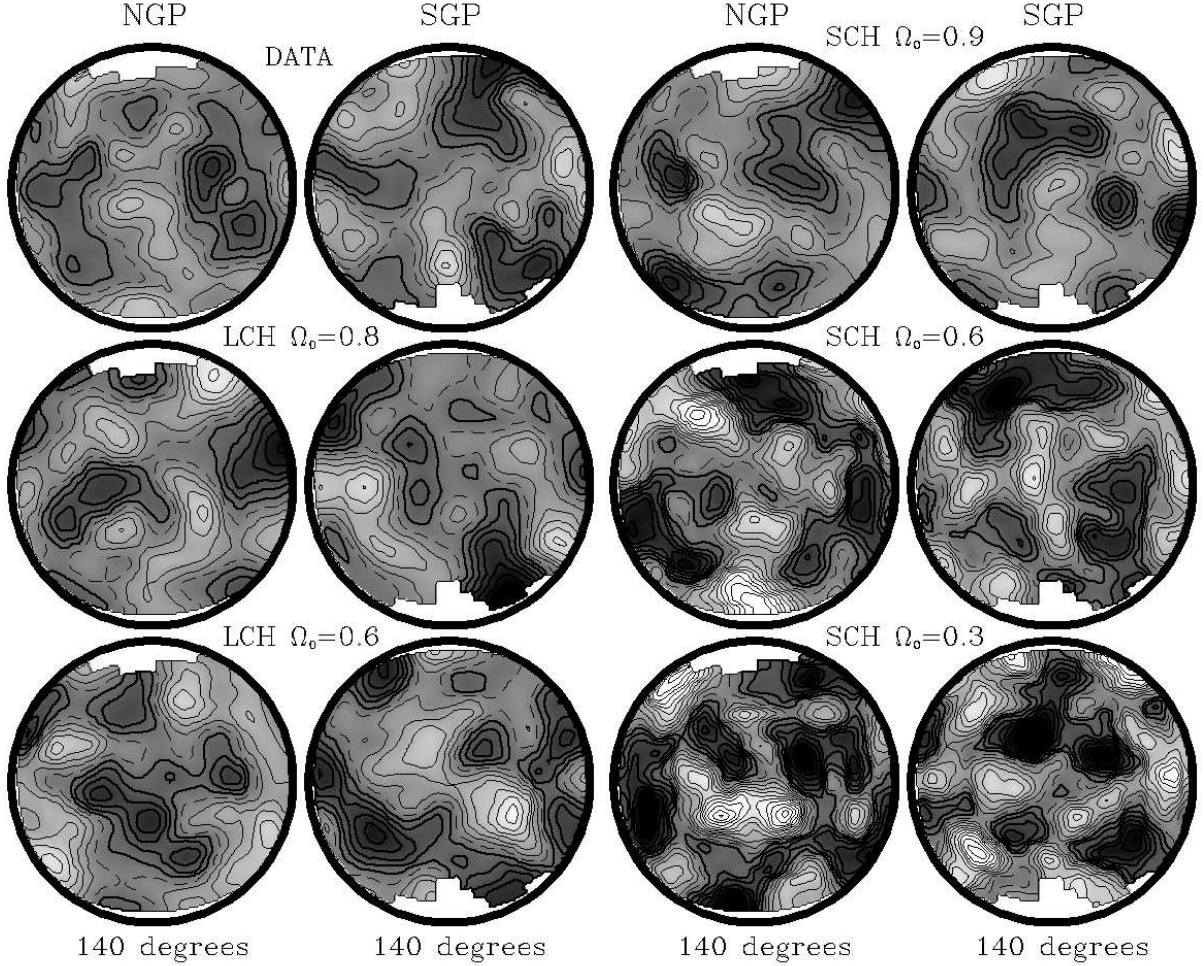


Figure 1: The figure consists of two columns of CMB sky-maps showing a pair of 140° diameter hemispherical caps each, centered on the South (SGP) and North (NGP) Galactic Poles, respectively. The map labeled DATA, shows the COBE-DMR 53+90+31 GHz A+B data after Wiener filtering assuming a standard CDM model, normalized to COBE. The rest of the five maps are one random realization of the CMB anisotropy in two examples of compact hyperbolic (CH) spaces for several values of Ω_0 based on our theoretical calculations of $C(\hat{q}, \hat{q}')$ convolved with the COBE-DMR beam. Both surface and integrated (ISW) Sachs-Wolfe effects have been included in $C(\hat{q}, \hat{q}')$. No noise was added. The power was normalized to best match the COBE data. The theoretical sky was optimally filtered using the COBE experimental noise to facilitate comparison with data. The maps labeled L(arge)CH refer to the CH model $v_{3543}(2, 3)$. The right column shows the CMB maps for the S(mall)CH model $m_{004}(-5, 1)$. (The model number associated with the topology corresponds to that of the census of CH spaces in the Geometry center, Univ. of Minnesota; SCH is one of the smallest and LCH is one of the largest spaces in the census). LCH with $\Omega_0 = 0.8$ is compatible with the data with a suitable choice of orientation while all the others are ruled out (See Table 1). For all six maps, the average, dipole and quadrupole of the $|b| > 20^\circ$ sky were also removed and a 20° Galactic latitude cut was used, with extra cuts to remove known regions of Galactic emission proposed by the COBE team accounting for the ragged edges. The contours are linearly spaced at $15 \mu\text{K}$ steps. The maps have been smoothed by a 1.66° Gaussian filter.